High-contrast inclusions in generalized out-of-plane problem

S. Shahzad, F. Dal Corso, D. Bigoni

Department of Civil, Environmental and Mechanical Engineering, University of Trento, Italy

Abstract

The rigid inclusion model predicting a singular stress field in an elastic plate , is validated for the first time via photoelastic experiments under mode I [1]. Results show that the stress concentrations near corners of stiff inclusions can reach very high values leading to catastrophic failure of structural components. In particular, for the case of rhombohedral rigid inclusion, it is experimentally observed a stress magnifaction factor 5.3.
Notch stress intensity factors are derived for matrix containing small voids and rigid polygonal inclusions subjected to remote self-equilibrated anti-plane shear load (mode III) described by a generic order polynomial, which is found to be dependent on two constants for each order. By means of Schwarz-Christoffel map in a differential closed-form expression [2], it is shown that (i) a complex potential governing the out-of-plane problem is given by a closed-form formula and (ii) the notch stress intensity factors are strictly related to the unperturbed stress state at the singular point ($\tau_{23}(a,0)$ for void and $\tau_{13}(a,0)$ for rigid, where "a" represents the distance between the corner point and the origin along x_1) and depends on the shape ofthe inclusion.

Asymptotic fields near a rigid wedge and near a notch

For the rigid wedge, similarly to the notch problem:

- the singularity appears only when $\alpha > \pi/2$;
- a square root singularity ($\sigma_{\alpha\beta} \sim 1/\sqrt{r}$) appears for both mode I and II when α approaches π (corresponding to the rigid line inclusion model, see [2]);

while, differently from the notch problem:

- the singularity depends on the Poisson's ratio ν through the parameter κ;
- the singularity under Mode II condition is stronger than that under Mode I.

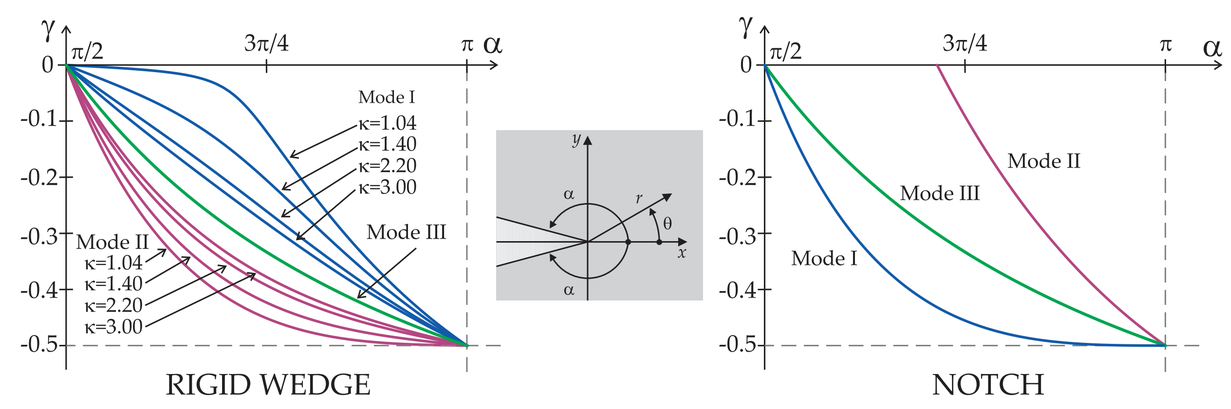

Fig. 1. Theoretical singularities at the tip of the rigid wedge (left, under plane strain) and of the notch (right) under Mode I, Mode II and Mode III loading conditions. The square root singularity depends on angle α.

Full-field solution and photoelastic results

The Full-field linear elastic solutions is obtained by complex potential method [1] via Conformal Mapping. Photoelastic fringe have been obtained through linear and circular polariscope at white and monochromatic light.

Comparison between analytical solution and photoelastic experiment

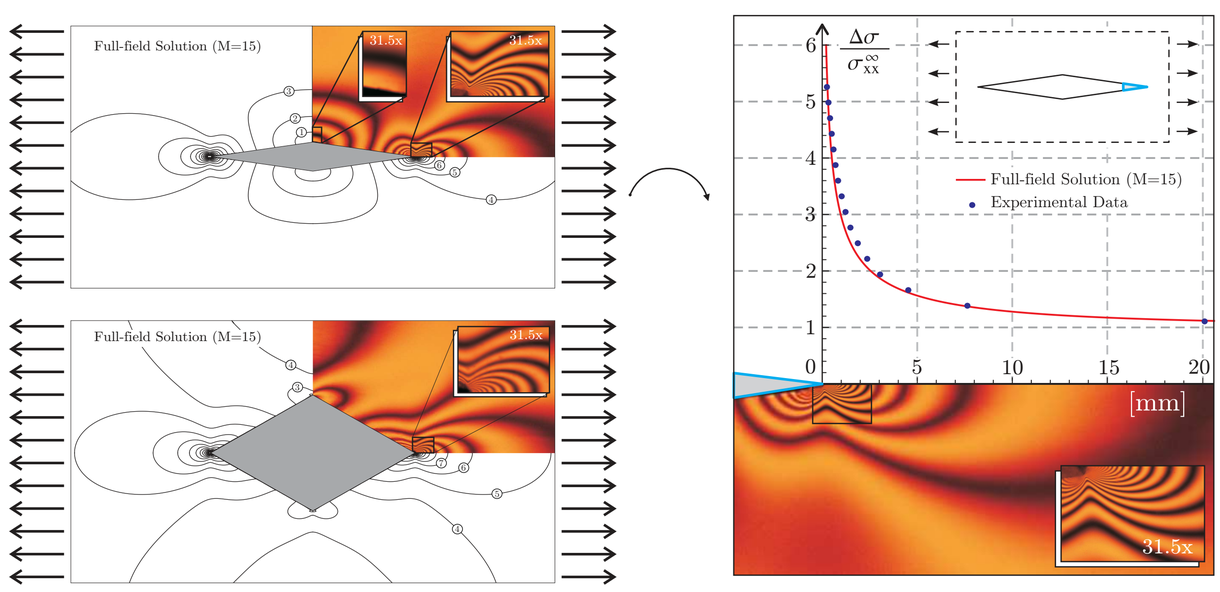

Fig. 2. Photoelastic fringes revealing the stress field near stiff rectangular and rhombohedral inclusions embedded in an elastic matrix and loaded with uniaxial tensile stress σ^{∞}_{xx}=0.27 Mpa, compared to the elastic solution for rigid inclusions (plane stress, with Poisson's ratio equal to 0.49). Magnification factor of 5.3 (right) obtained.

Stiffener Neutrality under Mode II

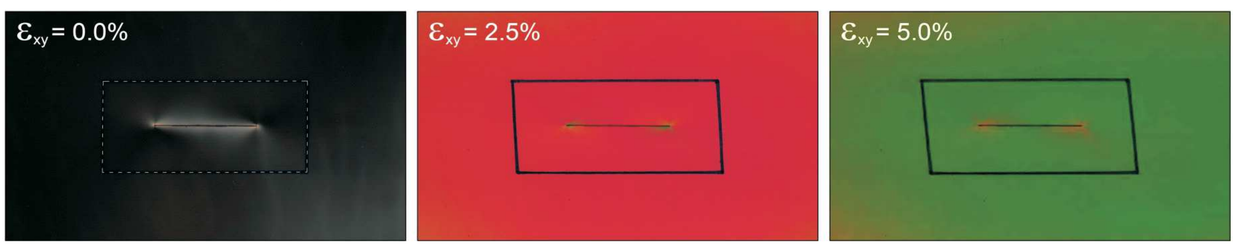

Fig. 3. Photoelastic fringes for in-plane principal stress difference around a stiffener subjected to a simple shear ($\varepsilon^{\infty}_{xy}$= { 0 ; 2.5 ; 5 } %) parallel to the inclusion line. The homogeneity of the fields demonstrates the stiffener neutrality [2].

Notch Stress Intensity Factor under Mode III

Generalize polinomial out-of-plane stress field

The generic polynomial antiplane stress field of p-th degree

$$\begin{cases} \tau_{13}^{\infty}(x_1,x_2) = \sum_{m=0}^{p} \tau_{13}^{\infty(m)}(x_1,x_2), \\ \tau_{23}^{\infty}(x_1,x_2) = \sum_{m=0}^{p} \tau_{23}^{\infty(m)}(x_1,x_2), \end{cases} \quad \text{with} \quad \begin{cases} \tau_{13}^{\infty(m)}(x_1,x_2) = b_0^{(m)} x_1^m + \sum_{j=0}^{m} c_j^{(m)} \dfrac{m-j}{j+1} x_1^{m-j-1} x_2^{j+1}, \\ \tau_{23}^{\infty(m)}(x_1,x_2) = \sum_{j=0}^{m} c_j^{(m)} x_1^{m-j} x_2^{j}, \end{cases}$$

NSIF for n-sided regular polygonal inclusions (m+1<n)

$K^{(m)}_{III}(n)$ and $K^{*(m)}_{III}(n)$ are notch stress intensity factor for void and stiff inclusions, respectively. Further $\Omega(n)$ represents the shape of regular polygons.

$$\begin{Bmatrix} K_{III}^{(m)}(n) \\ K_{III}^{*(m)}(n) \end{Bmatrix} = 2\sqrt{2\pi} \left(\frac{a\,\Omega(n)}{n+2} \right)^{\frac{2}{n+2}} (\Omega(n))^m \begin{Bmatrix} \tau_{23}^{\infty(m)}(a,0) \\ \tau_{13}^{\infty(m)}(a,0) \end{Bmatrix}$$

$$\Omega(n) = -\frac{1}{\pi} \sin\left(\frac{2\pi}{n}\right) B\left(\frac{n+1}{n}, -\frac{2}{n}\right) \in \left[\frac{1}{2}, 1\right]$$

where $B(\cdot,\cdot)$ denotes the Euler beta function.

NSIF for rhomboid shape polygonal inclusions (m+1<n)

$K^{(m)}_{III}(\beta)$ and $K^{*(m)}_{III}(\beta)$ are notch stress intensity factor for void and stiff inclusions, respectively. Further $\Omega(\beta)$ represents the shape of rhomboid type polygons.

$$\begin{Bmatrix} K_{III}^{(m)}(n) \\ K_{III}^{*(m)}(n) \end{Bmatrix} = \sqrt{2\pi} \left(\frac{2a\,\Omega(\beta)}{\beta} \right)^{1-\frac{1}{\beta}} (\Omega(\beta))^m \begin{Bmatrix} \tau_{23}^{\infty(m)}(a,0) \\ \tau_{13}^{\infty(m)}(a,0) \end{Bmatrix}$$

$$\Omega(\beta) = -\frac{\sqrt{\pi}}{2} \frac{\sec\left(\frac{\beta\pi}{2}\right)}{\Gamma\left(\frac{3-\beta}{2}\right)\Gamma\left(\frac{\beta}{2}\right)} \in \left[0.835, \frac{1}{2}\right]$$

where $\Gamma(\cdot)$ denotes the Euler gamma function.

Stiffener and Crack Neutrality under Mode III

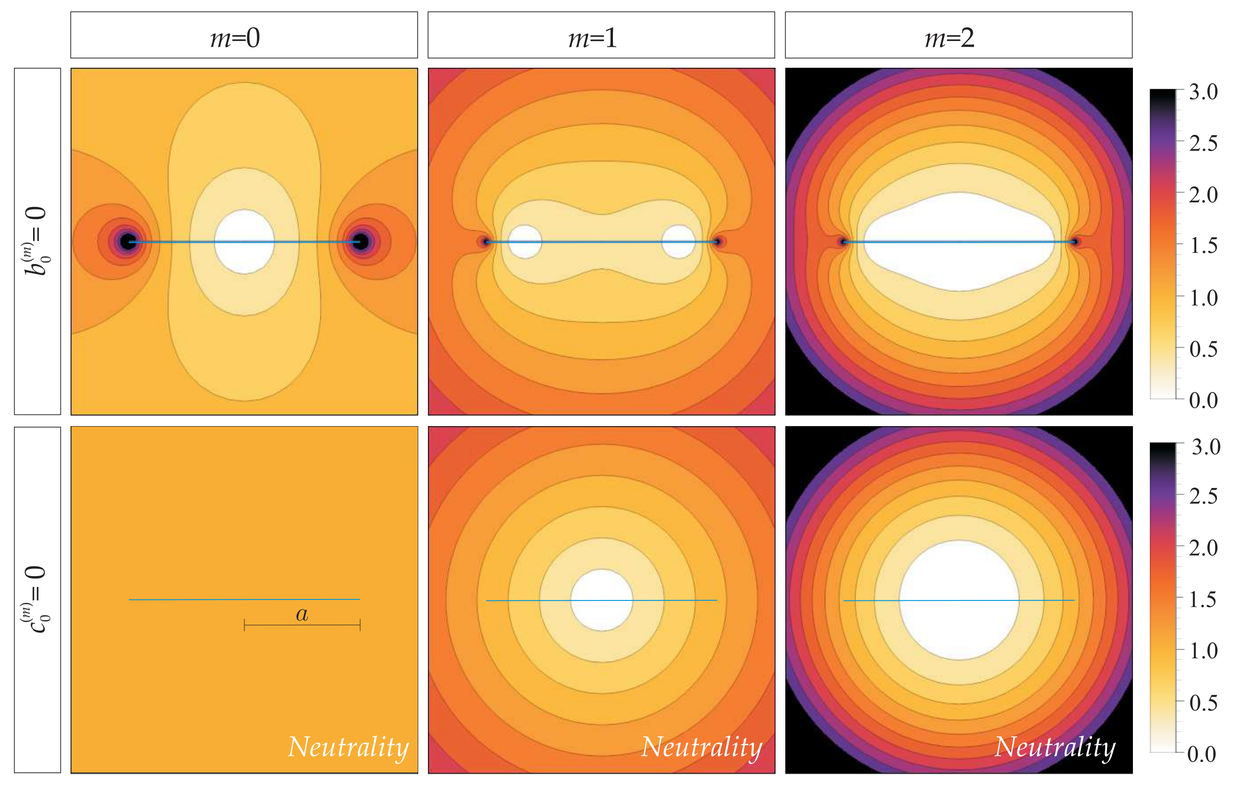

Fig. 4. Out-of-plane m^{th} order polynomial remote shear stress is applied to a elastic body containing a crack (upper part) and stiffner (lower part). Neutrality is obtained when the the shear stress is applied along x_1 for a crack and along x_2 for a rigid line inclusion. Where m=0,1,2 corrispond to a uniform , linear and parabolic antiplane shear loadings.

CONCLUSIONS

- The stress field near a stiff inclusion embedded in a soft matrix material can be effectively calculated by employing the rigid inclusion model.
- Close form formula for the notch stress intensity factors for polygonal void and rigid inclusions subject to a generalized polynomial antiplane shear load is obtained.
- Crack and Stiffner are found to be neutral under specific non uniform Mode III loadings .

REFERENCES

[1] D. Misseroni, F. Dal Corso, S. Shahzad, D. Bigoni, *Stress concentration near stiff inclusions: validation of rigid inclusion model and boundary layers by means of photoelasticity*, EFM 121–122 (2014) 87–97.

[2] Noselli, G., Dal Corso, F. and Bigoni, D. (2010). *The stress intensity near a stiffener disclosed by photoelasticity*. Int. J. Fracture, 166, 91–103.

[3] Kohno Y. Ishikawa H. *Singularities and stress intensities at the corner point of a polygonal hole and rigid polygonal inclusion under antiplane shear*. Int. J. of Eng. Sci. 1995; v. 33, Issue 11, p. 1547-1560.

ACKNOWLEDGMENTS

The authors gratefully acknowledge financial support from European Union FP7 project under contract number ERC-2013-ADG-340561-INSTABILITIES.